Catalysis Letters 13 (1992) 221–228

Methane oxidative coupling over Na_2WO_4/SiO_2

Q.J. Yan, Y. Wang, Y.S. Jin * and Y. Chen

*Department of Chemistry, * Material Analysis Center, Nanjing University, Nanjing, China*

Received 10 July 1991; accepted 15 January 1992

Methane oxidative coupling (MOC) was studied over Na_2WO_4/SiO_2. The effect of Na_2WO_4 loading and reaction conditions on the catalytic behaviour was investigated. XRD, SEM, LRS and XPS have been used to study the catalyst morphology, Na_2WO_4 dispersity and surface oxygen species. These results were correlated with the catalytic activity and selectivity.

Keywords: Oxidative coupling of methane; metal oxides; XRD; XPS; SEM; LRS; Na_2WO_4/SiO_2 catalyst

1. Introduction

At present, there is great interest in improving natural gas utilization. The oxidative coupling of methane has received considerable attention. A large number of metal oxides including reducible metal oxides, alkali metal ions promoted alkaline earth oxides and rare earth oxides have been tested and considerable progress has been made in elucidating the reaction mechanism [1–5]. Most researchers agree that the intermediate of oxidative dehydrodimerization of methane on oxide catalysts is $CH_3^{\cdot}$ radical and the formation of CO_x and C_2H_4 both take place heterogeneously and/or homogeneously [6]. Several authors have suggested that the catalytic activity and selectivity are related to the acid-base properties of the catalyst [7,8].

The purpose of this paper is to report a new type catalyst Na_2WO_4/SiO_2 which exhibits pretty good activity and selectivity for MOC. The catalytic performance will correlate with the catalyst morphology and surface state.

2. Experimental

Catalysts were prepared by the impregnation method. A specific amount of SiO_2 was added to aqueous solution of Na_2WO_4, the resulting slurry was stirred over a water bath at 333 K until dry and subsequently dried at 393 K for 12 hrs,

calcined in air at 1023 K for 5 hrs. The catalysts were pressed, crushed and sieved to a particle size of 20–40 mesh for use. The catalytic performance was carried out in a quartz fix-bed reactor with 40 mm I.D. Natural gas (> 95% CH_4) and air (99%) were used as feed gas and purified to remove sulfur and water before use. Pure CH_4 (99.9%) was also used instead of natural gas for comparison and gave a little decrease in C_2 yield. The reactants and products were analyzed by on line G.C. with 3 m molecular sieve 13X column for the analysis of N_2, O_2, CO and CH_4 and 3 m Porapak Q column for the analysis of CH_4, CO, CO_2, C_2 and C_3 hydrocarbons. The main products were C_2 hydrocarbons, CO_2, CO, H_2O, H_2 and small amounts of C_3H_8 and C_3H_6. Water was removed from the reaction products by a C_2H_5OH-L.N. trap before analysis. C_2 selectivity (%) is defined as

$$\frac{2X[(\text{moles } C_2H_4 + \text{moles } C_2H_6) \text{ in product}]}{\text{Total moles C in product}} \cdot 100$$

C_2 yield is defined as CH_4 conversion times selectivity.

A D/MAX-RA type X-ray diffractometer was used with Cu Kα radiation ($\lambda = 1.542$ Å) and a graphite filter for phase analysis. Raman spectra were measured using a Spex Ramanlog Model 1403 spectrometer with argon ion laser tuned to the 5145 Å line for excitation. The samples were mounted on a spinning sample holder. XPS experiments were carried out in a V.G. ESCALAB MKII system with a hemispherical analyzer operated at 20 eV. A Mg Kα X-ray source was used. C_{1s} (B.E. = 284.6 eV) was used as an internal standard to determine the binding energies of the other species. The catalysts morphology was characterized by a Hitachi X 560 type scanning electron microanalyzer.

3. Results and discussion

Table 1 shows the effect of Na_2WO_4 loading on the catalytic behaviour. The support SiO_2 itself shows fairly good activity for CH_4 conversion but poor C_2

Table 1
The effect of Na_2WO_4 loading on the catalytic properties of Na_2WO_4/SiO_2
$W = 0.3$ g, $T = 1073$ K, $F = 30$ ml/min, $CH_4/air = 1/2$

Na_2WO_4 loading (%)	$S_2A.$ (m^2/g)	Conversion (%)		Selectivity (%)				Yield (%)	
		O_2	CH_4	C_2H_6	C_2H_4	CO	CO_2	C_2	C_2H_4
0	242.8	95.3	27.3	2.7	7.3	77.7	12.3	2.7	2.0
2.5	20.6	77.8	26.6	10.3	21.6	46.2	22.0	8.5	5.7
5.0	4.3	94.7	33.2	15.1	37.7	21.0	26.2	17.5	12.5
10.0	2.3	85.1	32.7	13.8	43.4	22.8	20.0	18.7	14.2
20.0	2.0	69.0	26.9	12.2	41.8	32.1	13.9	14.5	11.2
40.0	2.0	46.8	18.4	16.1	36.4	35.1	12.4	9.7	6.7

Table 2
The effect of reaction conditions on catalytic activity and selectivity over 10 wt% Na_2WO_4/SiO_2

Space velocity (ml/g.hr)	CH_4/air	Conversion (%)		Selectivity (%)		Yield (%)	
		O_2	CH_4	C_2H_6	C_2H_4	C_2	C_2H_4
3000	1/2	95.1	37.8	14.6	43.7	22.0	16.5
6000	1/2	95.3	38.9	16.2	43.5	23.2	16.9
9000	1/2	83.6	37.0	19.1	43.3	23.1	16.0
3500	1/2.5	95.2	44.1	12.7	41.7	25.1	18.3
7000	1/2.5	91.9	44.5	14.6	41.7	25.1	18.6
3000	1/5	95.1	58.0	7.9	34.1	24.4	19.8
3000	1/1	95.2	23.1	22.4	47.6	16.2	11.0
3000	2/1	94.8	13.4	31.0	50.0	10.9	6.7

$T = 1093$ K.

selectivity. This characteristic may be partly related to the acid property and high surface area of SiO_2. Loading of Na_2WO_4 on the support causes significant increase of C_2 selectivity and a rather small increase of CH_4 conversion and also a decrease in the BET surface area. It seems that the role of Na_2WO_4 may simply be to reduce the specific surface area of the catalysts and to neutralize the acid sites on SiO_2. Since Na_2WO_4 is a base such scavenging of the residual acid sites on the SiO_2 surface is not novel. Little differences both in C_2 selectivities and the surface area of the catalysts were observed beyond 5% weight loading. This phenomen will be discussed later. The sample with 10 wt% loading gives the highest C_2 selectivity and yield.

Table 2 shows the effect of space velocity and CH_4/air ratio on the catalytic activity measured at 1093 K over the 10 wt% Na_2WO_4/SiO_2 sample. The selectivity of C_2H_6 increases with the increase of the space velocity that is with the decrease of the residence time of the feed gas on the catalyst. However, too high a space velocity will significantly decrease the conversion of O_2. Since the decrease of the CH_4/air ratio results in the increase of O_2 partial pressure and the partial pressure of N_2 as well, the methane conversion dramatically increases at the expense of the C_2 selectivity. When CH_4/air ratio is 1/2.5, a 44% CH_4 conversion and 41.7% C_2H_4 selectivity are obtained. With a CH_4/air ratio of 2, the selectivity of C_2 and C_2H_4 are 81% and 50% respectively, and the conversion of CH_4 decreases to 13.4%.

Tables 1 and 2 provide some insight on the C_2 and CO_x ($x = 1, 2$) formation mechanism. Since C_2H_6 selectivity decreases and C_2H_4 selectivity and CH_4 conversion remain virtually constant with the decrease of space velocity, we may suggest that further oxidation of C_2H_6 to CO_x does occur. As shown in table 1, a lower surface area gives a higher C_2 selectivity, it seems that the CO_x formation takes place mainly on the catalyst surface. In addition, the fact that the C_2H_4/C_2H_6 ratio varies with the Na_2WO_4 loading and increases with the

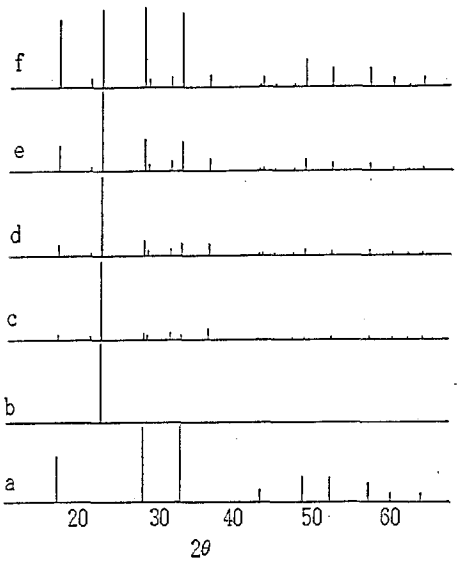

Fig. 1. XRD patterns of Na_2WO_4/SiO_2. (a). Na_2WO_4, (b). 2.5 wt% Na_2WO_4/SiO_2, (c). 5 wt% Na_2WO_4/SiO_2, (d). 10 wt% Na_2WO_4/SiO_2, (e). 25 wt% Na_2WO_4/SiO_2, (f). 40 wt% Na_2WO_4/SiO_2.

oxygen concentration in the feed gas reveals that the conversion of ethane to ethylene also occurs either in the gas phase or on the catalyst surface [9].

The effect of reaction temperature on CH_4 conversion and C_2 selectivity has also been examined over the 10 wt% Na_2WO_4/SiO_2 sample. Methane and oxygen conversion increase with increasing temperature up to 1073 K, no significant change is observed for C_2 selectivity. Beyond 1093 K, both C_2 selectivity and CH_4 conversion begin to decrease.

The bulk structure and the morphology of the catalysts were examined via XRD and SEM methods. XRD results show that in supported Na_2WO_4/SiO_2, the amorphous SiO_2 is transformed to α-cristobalite below 1023 K, its pore structure disappears and results in the dramatic decrease of the surface area (table 1). From fig. 1 we can see that the 101 face of α-cristobalite shows up in the 2.5 wt% Na_2WO_4/SiO_2 sample, but no Na_2WO_4 crystalline phase is detected by XRD. As the loading increases to 5 wt%, all other characteristic peaks of α-cristobalite appear and cubic Na_2WO_4 phase is also detected. Fig. 2 shows the SEM results. Similar morphology is observed for samples with 5, 10, 20 wt% Na_2WO_4 loading. The coral-like structure should be related to the interaction between Na_2WO_4 and SiO_2. When Na_2WO_4 content reaches 40 wt%, the sample's morphology is similar to that of crystalline Na_2WO_4. LRS results are given in table 3. The Raman spectra of Na_2WO_4 exhibit five characteristic frequencies at 930 cm^{-1} (symmetric W-O stretch), 814 cm^{-1} (antisymmetric W-O stretch), 376 and 312 cm^{-1} (W-O bending vibration) and 94

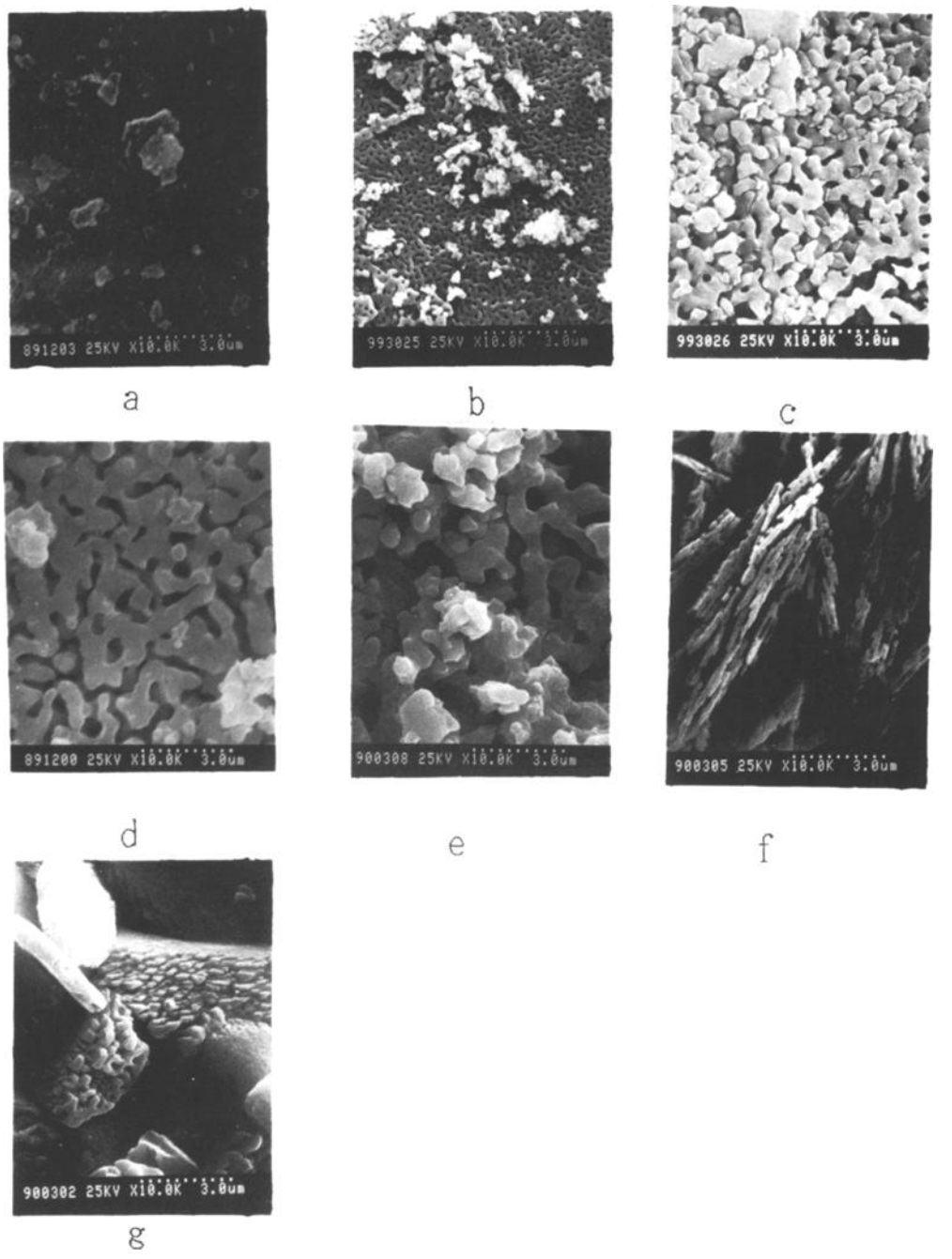

Fig. 2. SEM images of the samples. (a). SiO_2, (b). 2.5 wt% Na_2WO_4/SiO_2, (c). 5 wt% Na_2WO_4/SiO_2, (d). 10 wt% Na_2WO_4/SiO_2, (e). 20 wt% Na_2WO_4/SiO_2, (f). 40 wt% Na_2WO_4/SiO_2, (g). Na_2WO_4.

Table 3
Raman shifts of the samples

Samples	Raman shift (cm^{-1})
Na_2WO_4	94, 312, 376, 814, 930
2.5 wt% Na_2WO_4/SiO_2	458
5 wt% Na_2WO_4/SiO_2	226, 314, 418, 930, 958
10 wt% Na_2WO_4/SiO_2	114, 232, 314, 418, 812, 930, 958
40 wt% Na_2WO_4/SiO_2	116, 234, 314, 378, 420, 814, 930, 960

cm^{-1} (lattice vibration), respectively. No characteristic band of Na_2WO_4 is detected for the 2.5 wt% sample. As the loading is over 5 wt%, the major vibration of Na_2WO_4 is observed; but the lattice vibration band at 94 cm^{-1} can only be seen in the 40 wt% sample. When the loading is over 5 wt%, three additional bands are observed at 116, 226–234 and 958–960 cm^{-1}. The 226–234 cm^{-1} peak and 958–960 cm^{-1} peak could be assigned to W-O-W deformation and W-O symmetric stretching, respectively. It is believed that these bands are associated with two-dimensional surface tungstate species [10]. These results suggest that small Na_2WO_4 crystallites coexist with the highly dispersed and amorphous Na_2WO_4 on the surface of α-cristobalite at the loading range of 5%–20%. Table 1 indicates that the sample with 40 wt% loading gives only 18% CH_4 conversion, which is much lower than that over SiO_2 itself. We may conclude that the crystal Na_2WO_4 phase is not favourable to the CH_4 conversion, but the highly dispersed Na_2WO_4 and small Na_2WO_4 crystallites on the surface of α-cristobalite are benefit to the CH_4 conversion and C_2 formation.

The surface Na/Si atomic ratios determined by XPS are given in table 4. For all four catalysts, the Na/Si ratio at the surface is greater than that in the bulk, with the ratio of 0.49 being the greatest for the 10 wt% sample. This value is almost ten times greater than that in the bulk. It confirms that the surface of these catalysts are covered with highly dispersed Na_2WO_4. As an example of XPS spectra in the O_{1s} region, the O_{1s} spectrum of 10 wt% Na_2WO_4/SiO_2 is shown in fig. 3. Three peaks may be resolved, at binding energies of 532.9, 531.9 and 530.1 eV. Since the XPS spectra of SiO_2 and Na_2WO_4 show the O_{1s} peaks at 532.9 and 530.1 eV, respectively, we suppose that the O_{1s} peak at 531.9 eV

Table 4
Na/Si atomic ratio determined by XPS and C.A.

Na_2WO_4 loading (wt%)	Na/Si in bulk (C.A.)	Na/Si at surface (XPS)
2.5	0.010	0.17
5	0.022	0.32
10	0.044	0.49
20	0.100	0.36

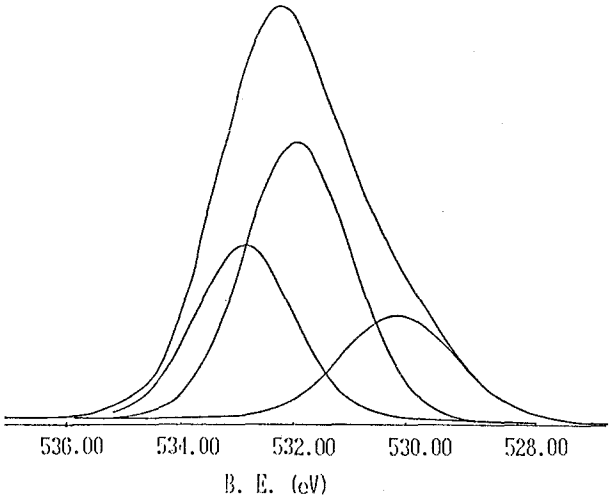

Fig. 3. O_{1s} spectrum of 10 wt% Na_2WO_4/SiO_2.

resulted from the interaction between Na_2WO_4 and SiO_2 and tentatively assigned to some kind of surface oxygen species.

It is generally accepted that methane activation is via abstraction of a hydrogen atom from methane by the catalyst. The O^- species is believed to be one of the active centers for abstraction of the hydrogen atom [1]. J.H. Lunsford and coworkers [11] suggested that the Li^+O^- species are responsible for the generation of $CH_3^{\cdot}$ radicals on Li/MgO. Otsuka et al. [12] suggested that O_2^{2-} could be the oxygen species responsible for methane activation over rare earth metal oxides and alkali metal promoted oxides. Osada et al. [13] suppose that O_2^- is one of the active sites on the Y_2O_3-CaO catalyst. It is well known that Na_2WO_4 is a complex oxide with a modified spinel structure. Our experimental results confirm that the transformation of SiO_2 to α-cristobalite is enhanced by Na_2WO_4. For the 10 wt% Na_2WO_4/SiO_2 catalyst, the high dispersion of Na_2WO_4, the enrichment of Na atoms and the formation of surface oxygen species with binding energy of 531.9 eV on the surface were observed. We suppose that those are responsible for the good catalytic property of the catalyst.

4. Conclusion

The Na_2WO_4/SiO_2 catalyst prepared by the impregnation method is active and selective for the oxidative coupling of methane. C_2 selectivity and yield of the catalysts at 1073 K increase remarkably by increasing the loading of Na_2WO_4 and reach a maximum at 10 wt%. The highest C_2 yield obtained at 1093 K with a CH_4/air ratio of 1/2.5 and a space velocity of 7000 ml/g.hr is 25.1%.

Highly dispersed and small crystallites of the Na_2WO_4 coexist on the support surface at the loading range of 5–20%. The most active sample has a coral like morphology, the highest Na/Si ratio on the surface and a surface oxygen species with binding energy of 531.9 eV.

Acknowledgement

The support of the National Natural Science Foundation of China is gratefully acknowledged.

References

[1] J.S. Lee and S.T. Oyama, Catal. Rev.-Sci. Eng. 30 (1980) 249.
[2] G.E. Keller and M.M. Bhasin, J. Catal. 73 (1982) 9.
[3] K. Otsuka, S. Yokoyama and A. Morikawa, Chem. Lett. (1985) 319.
[4] C.H. Lin, J.X. Whang and J.H. Lunsford, J. Catal. 111 (1988) 302.
[5] Y. Amenomiya, V.I. Birss, M. Goledzinowski, J. Galuszka and A.R. Sanger, Catal. Rev.-Eng. 32 (1990) 163.
[6] M.Yu Sinev, V.N. Korchak and O.V. Kryla, Kinet. Catal. 28 (1988) 1188.
[7] S.K. Agarwal, R.A. Migone and G. Marcelin, Appl. Catal. 53 (1989) 71.
[8] I.T. Ali Emesh and Y. Amenomiya, J. Phys. Chem. 90 (1986) 4785.
[9] G. Wendt, C.D. Meinecke and W. Schmitz, Appl. Catal. 45 (1988) 209.
[10] S.S. Chen, I.E. Wachs, L.L. Murrell and N.C. Dispenziere, J. Catal. 92 (1985) 1.
[11] J.X. Wang and J.H. Lunsford, J. Phys. Chem. 90 (1986) 5883.
[12] K. Otsuka and K. Jinno, Inorg. Chim. Acta. 121 (1986) 237.
[13] Y. Osada, S. Koike, T. Fukushima, S. Ogasawara, T. Shikada and T. Ikariya, Appl. Catal. 59 (1990) 59.
[14] A.F. Wells, *Structure Inorganic Chemistry* (Clarendon Press, Oxford, 1984).